This paper is part of the Proceedings of the 2nd International Conference on High Performance and Optimum Design of Structures and Materials (HPSM 2016)
www.witconferences.com

Ballistic resistance of various materials suitable for indoor bullet traps

F. Tikal & S. Špirk
Faculty of Mechanical Engineering, Regional Technological Institute, University of West Bohemia, Czech Republic

Abstract

The aim of this research was to identify optimum thicknesses for selected commercially available materials at several impact energies of bullets from ordinary civilian small arms. These impact energies are characteristic of certain bullet calibres and were selected from a survey of requirements of civilian ranges in the Czech Republic in cooperation with the IPSC National Association.

The research was motivated by the fact that bullet traps for indoor/tunnel civilian ranges are often designed on a case-by-case basis, disregarding the applicable principles of mechanical metallurgy, and lifetime and weldability aspects. To improve the trap performance, the metal structure is normally clad with rubber in the form of used tires, discarded conveyor belts, and similar items. These rubber parts must be frequently replaced. Their disposal together with the embedded bullets and bullet fragments is expensive and even poses environmental risks. Eliminating such rubber components altogether is another goal of this research.

In the first phase, terminal ballistic computer simulations were developed. Then, a set of experiments was proposed to verify the results of these simulations. The impact of a bullet was simulated on target plates of selected materials of various thicknesses at various target plate angles. An explicit FEM solver was employed for this purpose. Based on the simulation results, optimum combinations involving the impact energy/material/thickness/target plate angle were identified for experimental verification. Selected experiments were recorded by a high-speed camera and a high-speed thermal imaging camera. The results and knowledge acquired will enable the bullet and fragment trap design to be tailored to a specified

WIT Transactions on The Built Environment, Vol 166, © 2016 WIT Press
www.witpress.com, ISSN 1743-3509 (on-line)
doi:10.2495/HPSM160161

maximum bullet calibre, taking into account purchase and operating costs and, last but not least, environmentally-friendly operation without rubber components.

Keywords: special materials, computer simulation, experiments, terminal ballistics.

1 Introduction

A recent analysis of today's dynamic bullet trap constructions revealed an absence of standards and design guidance.

Ordinarily, general engineering design rules are applied to these devices without any analytical verification, let alone numerical simulations. A lack of knowledge of the characteristics of trap materials is commonplace. The safety and durability of the equipment are provided by merely overdesigning the structure by estimate. No attention is paid to optimum joint designs, and welded joints are employed without considering the durability of such a joint under dynamic impact loads.

Combinations with non-metallic materials, such as rubber in the form of discarded tires or conveyor belts, are commonly used. This results in high purchase costs, and expensive and environmentally-unfriendly operation of bullet traps.

The purpose of the present research was to systematically develop a suitable design, to map both conventional and special materials, and to verify their use under pre-selected defined loads. This was accomplished using both numerical simulations, and testing in practice.

A concept of an optimized dynamic bullet trap was verified using an explicit finite element solver. Explicit modelling enables extreme nonlinear behaviour to be simulated for extreme situations which are at or beyond the limits that the conventional FEM programmes can handle.

Dynamic tests on selected materials were carried out to acquire input data for numerical simulations. Impact simulations were then conducted, accounting for the effects of bullet penetration. The resulting degree of protection was evaluated from the simulation results with respect to the material and orientation and damage of the target plates. To validate the bullet trap concept, a series of experiments was conducted on a test stand under real-life conditions.

2 Conditions statement

In the first step of mapping the requirements for the bullet trap, statistics were compiled on the basis of regional requirements. The most common limit calibres or, more precisely, bullet energy levels were identified for civilian long firearms. Materials [1] were selected with regard to the intention to employ sandwich structures in the future. For the numerical simulations, the bullet velocity and energy levels were defined for the firing distances reported by manufacturers as experimental testing conditions.

3 Boundary conditions

3.1 Cartridge type

The cartridges used were SAKO .308 Win 141A Racehead. The bullet type was Racehead HPBT, a lead-core full metal jacket bullet weighing 10.9 grams. This bullet stands out thanks to its very thin jacket and boat tail-shaped bottom, which provides it with very good ballistic characteristics.

3.2 Materials and dimensions of specimens

The dimensions of the specimens of materials were 210×297 mm.

a) Hardox 500 plate with a thickness of 8 mm.

This is an abrasion-resistant steel with a hardness of about 500 HB, made by SSAB Oxelösund, Sweden. Hardox 500 is not intended for further heat treatment. It obtains its mechanical properties by quenching and is not suited to applications with temperatures above 250°C. After such exposure, the material may lose its intended properties. Welding of this material is not recommended.

b) S355 steel (Czech Standard designation CSN 11523) with thicknesses of 10 mm and 12 mm.

This is a plain carbon structural steel. This material has good weldability.

3.3 Test setup

Rake angles of specimens on the stand: 90° and 45° to the horizontal axis.
Firing distance: 50 metres.

4 Numerical simulation

4.1 Theory of explicit FEM modelling

The beginnings of the development of explicit solvers date back to the 1960s. At that time, such development took place mainly at universities. The HEMP program, whose code was freely accessible, became the basis for today's software packages. Explicit time integration is suitable for simulating processes which involve large strains and changes in shape. It offers better representation of the nonlinear behaviour of materials, and failures. Explicit solvers are generally better suited for problems with complex contact situations. Therefore, they are a good choice for solving collision problems, crashes, bullet penetrations, and similar tasks.

The essence of an explicit code is Newton's second law of motion. It is an equation of motion in the matrix form (1). This equation is defined for the given time instant. In order to maintain equilibrium between dynamic forces, the relationships below must be met [2].

$$\{a_t\} = [M]^{-1}\left(\{F_t^{ext}\} - \{F_t^{int}\}\right) \quad (1)$$

Here, $\{a_t\}$ denotes the acceleration vector (at time instant t), $[M]$ is the mass matrix, F_t^{ext} stands for the vector of external forces acting on the body, and F_t^{int} is the vector of internal forces.

Once the internal forces have been defined and some fundamental elements added, an equation for the numerical solution can be obtained in the following form (2). The element $\{F^{houg}\}$ was added to prevent the hourglassing effect, and $\{F^{cnt}\}$ is a vector of contact forces. Furthermore, $\{\sigma_n\}$ is an internal stress matrix, and $[B]$ is a strain matrix.

$$\{F_t^{int}\} = \sum \left(\int_\Omega [B]^T \{\sigma_n\} d\Omega + \{F^{houg}\} \right) + \{F^{cnt}\} \tag{2}$$

Solvers that use the explicit code are conditionally stable. This means that they are only stable under certain conditions, referring mainly to the time step size. This, in turn, is related to the propagation of stress waves through the material (see the following equation (3)). Here, c is the velocity of the wave propagating through the material, l is the characteristic size of an element, E is the modulus of elasticity, and ρ the density of the material.

$$t_{calc} \leq t_{krit} = \frac{l}{c} = l\sqrt{\frac{\rho}{E}} \tag{3}$$

A great advantage of the explicit method is the use of elements with a single integration point. A downside is the reduced stability of computation. If an element deforms symmetrically, no corresponding change in internal energy takes place. Eventually, the computation leads to an imbalance between the kinetic and the internal energy of the system. This numerical error is known as hourglassing. Clearly, the total energy must be controlled in dynamic calculations. The recognized critical threshold is an increase in the hourglassing energy above 5% of the total energy of the system. In extreme cases with a severe hourglassing effect, the simulation run may even crash. Various methods are available to control hourglassing.

4.2 PAM-CRASH: explicit FEM solver

PAM-CRASH is an FEM solver which is part of the software package VPS (Virtual Performance Solution) from ESI Group [2]. The software is used for crash simulations and safety assessment, most often in the automotive industry.

Its development has continued since 1978 and is connected with the early car crash simulations. Based on the finite element method (FEM), it supports complex-geometry models with a variety of element types. It also offers a wide range of linear and nonlinear materials, including visco-plastic, foam and multi-layer composites, and failure models [4].

As it relies on the explicit formulation in FEM, it is suitable for nonlinear problems with large numbers of contacts (relying mainly on the penalty algorithm).

This software was selected on the basis of references from the defence sector and its ability to solve problems involving the performance of munitions with respect to explosion, cratering, and simulation of kinetic energy penetrators.

4.3 Description of numerical simulations

First, a simulation model was constructed. Boundary conditions were defined, and material data from dynamic tests implemented.

The goal was to carry out computer simulations of bullet impacts on steel target plates. The problem was formulated using the PAM-CRASH software and the explicit integration scheme. The 3D geometry model was developed using the NX 9.0 program, based on a longitudinal section through the bullet. In this section, all relevant dimensions, including the jacket thickness, were measured.

In contrast to the manufacturer data, the weight of the entire bullet was found to be 12.3 g. This includes the lead core and the bronze jacket. Densities of these materials were found in literature and corrected according to the readings using the following simple relationship.

$$m_{bullet} = (m_{core} + m_{jacket}) \cdot c = c\rho_c v_c + c\rho_j v_j \tag{4}$$

Here, m_{bullet} is the actual weight of the bullet, m_{core} denotes the core weight, m_{jacket} is the jacket model weight, and c denotes the ratio of actual and model values.

The bullet velocity was determined from empirical relationships based on the amount of gunpowder and the distance travelled by the bullet. It was verified using a bullet velocity calculator available on the manufacturer's website [5]. The impact velocity is taken as 779 m/s. The bullet spin was derived from the parameters of the barrel. The twist rate of the 308-calibre Winchester rifle is 1:12". Hence, the bullet completes one full revolution in a path of 304.8 mm. At the above velocity, the bullet completes 2.56 revolutions in a millisecond, making a rotation speed of 16.08 rad/ms.

The failure criterion used here involved maximum plastic strain and was implemented by element elimination. The critical time step was defined on the basis of the characteristic element size, Young's modulus and stiffness: $\Delta t=8.9e^{-6}$ ms. The simulated process duration was 0.14 ms.

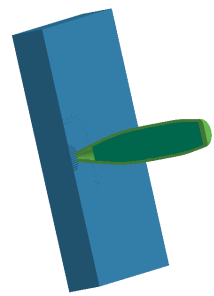

Figure 1: Sectional view of the 3D problem geometry.

4.4 Material models

The pressure-volume behaviour was defined by a polynomial equation of state. In the equation, the pressure p was a function of the parameter μ.

$$p = C_0 + C_1 \cdot \mu + C_2 \cdot \alpha \cdot \mu^2 + C_3 \cdot \mu^3 + (C_4 + C_5 \cdot \mu + C_6 \cdot \mu^2) \cdot E_i \qquad (5)$$

Here, $\mu = \rho/(\rho_0 - 1)$, C_0 .. C_6 are material constants, E_i denotes internal energy and the coefficient α equals zero when $\mu < 0$. Some of the material constants can be derived from fundamental properties of the material, such as volume compressibility, whereas others can be modelled on equivalent terms of the relevant shock equation of state [6]. A comparison between the shock and polynomial equations of state is given in paper [7] as one of its topics.

The plastic behaviour is defined by the Johnson-Cook model [8]. The stress equation is as follows.

$$\sigma_y = \left(C_A + C_B \cdot \varepsilon_P^{C_N}\right) \cdot (1 + C_C \cdot ln\dot{\varepsilon}).(1 - T^{CM}) \qquad (6)$$

Here, $T = (T - T_{room})/(T_{melt} - T_{room})$, T_{room} denotes ambient temperature, T_{melt} is the melting temperature, ε_P is the equivalent plastic strain, $\dot{\varepsilon}$ denotes dimensionless plastic strain, and C_A , C_B, C_N , C_C and C_M are the Johnson-Cook model coefficients for the particular material, which are available in literature [9].

The first failure criterion employed was the maximum plastic strain criterion for element elimination. When the limit value is exceeded, the particular element is practically eliminated by reducing its modulus of elasticity to a negligible value. The limit value is dictated by the properties of the material in question.
The second failure criterion involved the deviatoric stress tensor. This criterion does not affect the volumetric dependence of stress on strain. The total stress is found from the following equation.

$$\sigma = \left(1 - d\left(\varepsilon_p\right)\right)\sigma_o \qquad (7)$$

Here, σ is the damage full stress tensor, $d\left(\varepsilon_p\right)$ denotes the isotropic scalar damage function, and ε_p represents plastic strain.

This simulation model is valid for one set of boundary conditions. Other models were created as variants of it derived by modifying this refined pilot model.

The bullet, consisting of a lead core and a brass jacket, hits a plate of S355 steel of 10 mm thickness. To create the appropriate model, we used linear quadratic elements with eight nodes. The average size of the elements was about 0.5 mm. Material model no. 19, denoted as “elastic-plastic-with-damage-failure”, was chosen as the representative configuration.

Models of all three materials were defined on its basis.

4.5 Calculation of material model data using JMatPro

JMatPro is a commercial software package which is based on the CalPhaD (Calculation of Phase Diagrams) methodology and extended by various models which allow calculation of materials' properties. It is now widely used in the steel industry and for obtaining material property data for FEM simulations [10].

It was employed for calculations of stress-strain material curves at various strain rates. These are often referred to as flow-stress curves in the steel industry. The input data for calculating the flow stress includes the chemical composition of the material and information about one of its basic mechanical properties (yield strength, ultimate strength, hardness) or grain size. These input data were measured on the following devices: ZEISS EVO25 with an Oxford Instruments detector (chemical composition) and WOLPERT Vickers hardness tester 432-SVD (hardness). The results are given in Table 1. The balance of the chemical composition consists of iron and deleterious residual elements.

JMatPro provides good results for general steels and wherever stress-strain curves are quickly needed. The results are plotted in Figure 2. Material models prepared by using JMatPro can be refined with the aid of the DEFORM FEM software, which is suitable for simulating metalworking processes. This comprehensive approach introduces the process history into the material model, which can thus be used by various simulations, such as the simulation of impact.

Table 1: Results of chemical analysis and hardness testing.

Material	Chemical composition				Hardness
	C %	Cr %	Mn %	Si %	
Hardox 500	0.25	0.60	0.70	0.30	52 HRC on the surface, 42 HRC below the surface
S355	0.10		1.50		157 HV

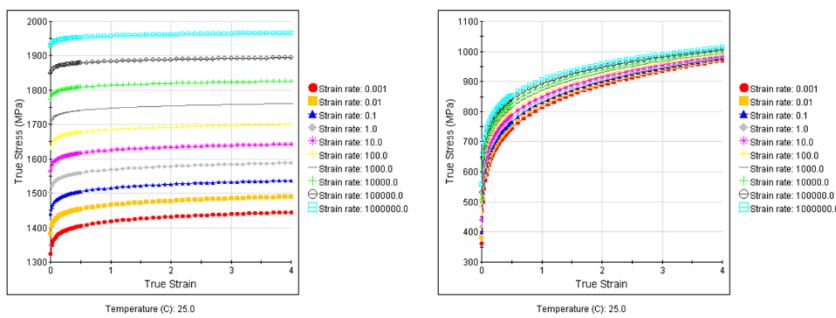

Figure 2: Material models: Hardox 500 (left) and S355 (right).

4.6 Results of numerical simulations

The simulation gives a good picture of the resistance of a steel plate. In the figure below, the formation of the hole at the point of entry of the bullet is clearly shown. Bullet penetration occurs in the plate with a thickness of 10 mm positioned at right angles to the bullet trajectory. The bullet velocity falls by 70% due to the loss of energy upon complete penetration.

The simulated impact of a bullet on a plate inclined at an angle of 45° with respect to the bullet trajectory does not lead to bullet penetration. This is in agreement with experimental results. The plate inclination significantly increases its resistance.

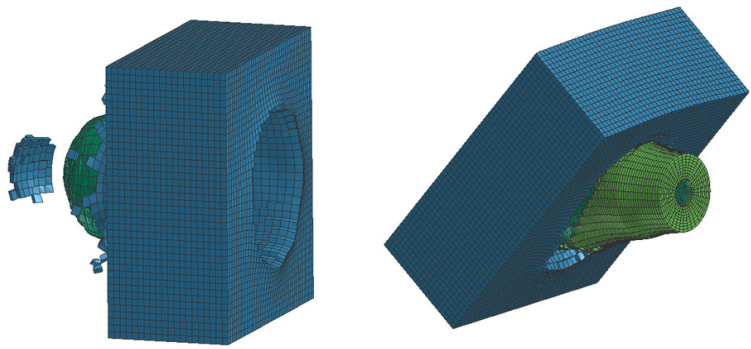

Figure 3: Results of the simulations – the plate from S355 material with a thickness 10 mm inclined at angles of 90° and 45°.

5 Experiments

To validate the numerical simulations, a series of experiments on a test stand under real operating conditions was carried out. The firing distance was 50 m and a sniper rifle of the following parameters was used:

Remington 700 Police (short action) [11] Calibre 0.308 Win. Barrel length: 26", standard twist: 12".

The experiments were conducted on specially made rectangular plates 210×297 mm in size fixed in a special stand. The angle of their inclination could be varied. There were two shots per each plate material and each angle. Each point of impact was documented, as shown in Figure 4.

Figure 4: Results of experiment – impacts at the angle of 90° are at the top of the plates, and those at 45° at the bottom.

The results of the experiment confirmed the calculated ballistic resistance of the plates. They are summarized in Table 2.

Table 2: Results of experiments.

Material	Angle	Thickness	Results for 2 shots
S355	90°	10 mm	penetration
S355	90°	12 mm	cup deformation
Hardox 500	90°	8 mm	micro deformation
S355	45°	10 mm	cup deformation
S355	45°	12 mm	cup deformation
Hardox 500	45°	8 mm	abrasion only

Selected experiments were recorded using a FASTCAM SA-X2 high-speed camera and a FLIR SC 7550 high-speed thermal imaging camera. The latter is a highly flexible camera with superior sensitivity, accuracy, spatial resolution and speed. It is specially designed for applications in science, industry, research and development.

6 Conclusion

In this study, the results of numerical simulations were verified by experiments. The findings will facilitate the selection of materials and the design of an optimized dynamic bullet trap. Generally, the results of simulations and experiments are in good agreement in terms of bullet penetration at particular

thicknesses, and target angles. However, the geometry of bullet holes differs between the simulations and experiments. An effort will be made to eliminate these discrepancies in the future [12].

The future research will cover more calibres, target plate angles and thickness values [13]. Additional materials will be selected for investigation on the basis of their price. Development and use of special rolled sandwich materials is anticipated.

The ballistic experiment setup will include an electronic chronograph to measure the bullet velocity. In addition, a high-speed camera and a high-speed thermal imaging camera on the test stand will be employed again to evaluate the dynamic impact process along with temperature monitoring.

Acknowledgements

The present contribution was prepared under project no. LO1502 'Development of the Regional Technological Institute', conducted under the auspices of National Sustainability Programme I of the Ministry of Education of the Czech Republic aimed at supporting research, experimental development and innovation.

References

[1] Hub, J., Komenda, J., *Ballistic Resistance of Steel Plate Hardox upon Impact of Non-Penetrating Projectiles*, Advances in Military Technology Vol. 4, No. 2, December 2009, pp. 79–91.

[2] Belytschko, T., Lin, J. L., Tsay, C.S., *Explicit algorithms for the nonlinear dynamics of shells,* Computer Methods in Applied Mechanics and Engineering 42 (1984), pp. 225–251.

[3] *Impact and high-velocity impact,* www http://virtualperformance.esi-group.com/applications-impact-and-high-velocity-impact-analysis (29. 04. 2015).

[4] Mestreau, E., Lohner, R., *Airbag Simulation Using Fluid/Structure Coupling*, 34th Aerospace Sciences Meeting & Exhibit, Reno, NV, January 1996.

[5] *Sako Ballistics* [WWW] http://luoti.sako.fi/Ballistics/index.jsp (29. 04. 2015).

[6] Steinberg, D. J., *Equation of State and Strength Properties of Selected Materials,* Lawrence Livermore National Laboratory report UCRL-MA-106439, 1991.

[7] Churilova, M., *Technology of EHIS (stamping) applied to production of automotive parts,* Department of Applied Mathematics. [Accessed 2016-04-15], www https://billionbooksbaby.org/pdf-stamping-through-mathematics.html.

[8] Johnson G. R., Cook W. H., *A Constitutive Model and Data for Metals Subjected to Large Strains, High Strain Rates and High Temperatures*, Proceedings of the 7th International Symposium on Ballistics, 54 (1983), p. 1.

[9] Borvik T., Deya S., Clausen A. H., *Perforation resistance of five different high-strength steel plates subjected to small-arms projectiles,* International Journal of Impact Engineering 36 (2009) 948–964.
[10] Diekmann, U., *Calculation of steel data using JMatPro*, COMAT2012, 21. – 22. 11. 2012, Plzeň, Czech Republic.
[11] *Remington 700 Police,* www http://www.remingtonle.com/rifles/700p.htm (29. 04. 2015).
[12] Buchar, J., Voldřich, J., *Terminal ballistics* (*in Czech*), Praha: Academia, 2003, ISBN 80-200-1222-2.
[13] Hub, J., Komenda, J., *Determination of the Protective Barrier Thickness of the Restraint System*, Advances in Military Technology Vol. 8, No. 2, December 2013, pp. 63–70.